Available online at www.sciencedirect.com
SCIENCE DIRECT®
Journal of Organometallic Chemistry 689 (2004) 1746–1756
Journal of Organometallic Chemistry
www.elsevier.com/locate/jorganchem

Coordination polymers and supramolecular structures in Ag(I)triflate–dppf systems (dppf = 1,1′-bis(diphenylphosphino)ferrocene) ☆

Xiu Lian Lu, Weng Kee Leong, T.S. Andy Hor *, Lai Yoong Goh *

Department of Chemistry, National University of Singapore, 3 Science Drive 3, Singapore 117543, Singapore

Received 16 December 2003; accepted 23 February 2004

Abstract

The interaction of silver triflate ($OTf^- = SO_3(CF_3)^-$) and dppf [$(C_5H_4PPh_2)_2Fe$)] gave different complexes, depending on the stoichiometric proportions and reaction conditions. Under limiting dppf conditions, three different forms (**1**–**3**) of $[Ag_2(OTf)_2(dppf)]_x$ were isolated. Single crystal X-ray diffraction analyses showed that the structure of **1** ($x = 2n$) consists of a 2-D polymer comprising a tetra-silver basic unit, while that of **2** ($x = 2$) possesses a discrete tetra-silver framework and that of **3** ($x = n$) is a linear polymer based on a di-silver repeating unit. The structures are supported by bridging dppf ligands and triflate groups. The crystal lattices of the compounds are stabilized by extensive intermolecular C–H···X hydrogen bonding (H = ring proton of Cp or Ph of dppf; X = O or F of OTf). [Ag(dppf)(OTf)] (**4**) and the structurally characterized mononuclear $[Ag(dppf)_2](OTf)$ (**5**) were the sole products obtained from treatment of AgOTf with dppf in molar ratios of 1:1 and 1:2, respectively.

Keywords: Coordination polymers; Supramolecular structures; Hydrogen-bonding; dppf ≡ 1,1′-bis(diphenylphosphino)ferrocene; Silver triflate

1. Introduction

The chemistry of supramolecular network structures, nanostructures and coordination polymers has attracted intense interest in recent years. The architecture of these structures is strongly influenced by the nature of the mediating metal and ligand, reaction stoichiometry, and counterions, and subtly by lattice solvate, intermolecular forces such as H-bonding and π–π stacking interactions [1,2]. Among the metals, silver and gold are of particular interest on account of the potential of their compounds as biologically active agents [3], catalysts [4] and luminescent materials [5]. The bulk of work on the supramolecular chemistry of silver utilized N, O or S donor bridging ligands [1c–1h,2]. Phosphine complexes of silver though extensively studied in coordination chemistry [5–7], have rarely featured in supramolecular assemblies, until very recently when a few polymeric and network assemblies were reported of complexes containing diphosphines with N-donor coligands [8a,8b,8c] and the bulky tris(2-furyl)phosphine [8d]. Notably unexplored is the role of metallodiphosphines, e.g. 1, 1′-bis(diphenylphosphino)ferrocene (dppf) [6] in supramolecular chemistry. It would be of interest to investigate the chemistry of silver complexes containing dppf with a potentially multidentate coligand like the triflate anion ($OTf^- = SO_3CF_3^-$). Recent work by Moore and coworkers had shown that in association with diphenylacetylenes, OTf has exhibited diverse coordination modes at silver, varying from monodentate via one oxygen atom forming cyclic dimeric structures or infinite structures of "half-bow-tie" chains, through bidentate bridging via two oxygen atoms forming infinite sheet structures [2i,2j] to μ_4-bridging via three oxygen atoms to four Ag atoms forming an infinite undulating sheet structure [2j]. This paper reports results from the reaction of Ag(OTf) with dppf.

☆ Supplementary data associated with this article can be found, in the online version, at doi:10.1016/j.jorganchem.2004.02.022.

* Corresponding authors. Tel.: +65-68742677; fax: +65-67791691.
E-mail addresses: andyhor@nus.edu.sg (T.S. Andy Hor), chmgohly@nus.edu.sg (L.Y. Goh).

0022-328X/$ - see front matter © 2004 Elsevier B.V. All rights reserved.
doi:10.1016/j.jorganchem.2004.02.022

2. Results and discussion

2.1. Reactions of Ag(OTf) with dppf

The reaction of Ag(OTf) and dppf *in 3:1 molar equivalents* in $CHCl_3$ *for 1.5 h* gave a yellow suspension; separation of the soluble and insoluble components followed by crystallisation gave the coordination polymers **1** (64%) and **3** (34%), respectively, both possessing the same stoichiometric $[Ag_4(OTf)_4(dppf)_2]$. The same reaction *for 20 h* again led to the isolation of **3** in identical yield (34%), together with a tetrameric complex $[Ag_4(OTf)_4(dppf)_2]$ (**2**) (62%) from the filtrate. **2** was also obtained (in 72% yield) from a 15 h reaction using *2 Ag(OTf):1 dppf* in MeOH–THF.

Crystallisation of **1** and **3** in CH_2Cl_2–hexane mixtures gave diffraction-quality crystals of the solvates, $\mathbf{1}\cdot 0.5CH_2Cl_2$ and $\mathbf{3}\cdot 0.5CH_2Cl_2$, respectively. Diffraction-quality crystals of **2** were obtained as $\mathbf{2}\cdot CH_2Cl_2$ (**2A**) and $\mathbf{2}\cdot 0.25CH_2Cl_2$(**2B**) by slow evaporation of a CH_2Cl_2 solution and from a CH_2Cl_2–hexane mixture, respectively.

Using 1 Ag(OTf):1 dppf, the reaction in CH_2Cl_2–toluene for 8 h gave in 90% yield a yellow solid (**4**), possessing an empirical formula [Ag(dppf)(OTf)], the structure of which is hitherto unknown.

Using 1 Ag(OTf):2 dppf the reaction in MeOH–THF for 8 h led to the isolation of $[Ag(dppf)_2](OTf)$ (**5**) as a yellow solid in 90% yield. Diffraction-quality crystals were obtained from CH_2Cl_2.

3. Spectral characteristics

NMR spectral characteristics of all the complexes are given in Table 1. IR and MS spectral data are given in Table S1 in Supplementary Information. Parent ions are not observed in the mass spectra. In the ES–MS of **3**, mass fragments (the highest being $[Ag_6(OTf)_5(dppf)_3]^+$) indicative of the presence of polymeric species were observed.

In the proton NMR spectra, the α and β protons of the Cp rings of dppf appear as two singlets in the region δ 4.19–4.72 in d_6-acetone, with slight shifts occurring when the temperature is lowered. At ambient temperature, the $^{31}P\{^1H\}$ spectrum of complexes **1**–**3** each shows a broad signal ($v_{1/2}$ 200–300 Hz) at ca. δ 5–7, which transforms into a sharp pair of doublets at 243 K and below, arising from coupling to $^{107/109}Ag$, with J values (710–820 Hz) indicative of coordination of one P atom per Ag center [9]; this is in agreement with X-ray structural analyses.

It is observed that the VT-^{31}P NMR spectral features vary significantly with solvent, as shown in Table 1 and illustrated in Fig. 1 for the compound **2** in d_6-acetone and in $CDCl_3$. It is significant that the low temperature doublets are much sharper in $CDCl_3$ and the broad virtual triplet in $CDCl_3$ at 300 K (δ 3.6, 6.4, 9.4, unres., each with $v_{1/2}$ ca. 300 Hz) is seen in d_6-acetone only as a broad peak δ 6.0 ($v_{1/2}$ 200 Hz). The chemical shifts of the ^1H(Cp) and ^{19}F resonances of **2** are also different in the two solvents. The VT features in the ^{31}P spectra can be rationalized based on *inter*- and *intra*-molecular exchange of ^{31}P with ^{107}Ag and ^{109}Ag, first observed by Dean and coworkers in dinuclear Ag complexes containing bridging diphosphines [10].

Complexes **4** and **5** exhibit slightly different VT features in their ^{31}P spectra. At 300 K, both exhibit a broad doublet, which at low temperature (223 K) shows coupling to $^{107}Ag/^{109}Ag$. The magnitude of these couplings (**4** 401/465 Hz, and **5** 232/271 Hz) is in agreement with the coordination of two and four P atoms, respectively, per Ag center [9], as evident in their chemical formulae and also confirmed by structural analysis in the case of **5**.

Table 1
NMR spectral data[a]

Complex	^1H δ (Cp) of dppf[b]		$^{31}P\{^1H\}$		^{19}F δ	
	300 K	223 K	δ ($v_{1/2}$, Hz), 300 K	δ ($J^{107/109}$ Ag–P, Hz)[c], 223 K	300 K	223 K
1	4.41, 4.61	4.22, 4.69	5.5 (ca. 300)	5.2 (714, 820)	−1.9	−2.3
2	4.43, 4.55	4.25, 4.67	6.0 (ca. 200)	5.3 (710, 820)	−1.9	−2.3
2[d]	3.87, 4.55	–	3.6, 6.4, 9.4 (unres., ca. 260, 300, 260)	–	−1.6	–
3	4.41, 4.60	4.23, 4.69	5.3 (ca. 200)	5.2 (714, 820)	−2.0	−2.4
4	4.38, 4.57	–	−0.9 (d, br, J_{Ag-P} 424 Hz)	−2.0 (401, 465)	−2.7	–
5	4.19, 4.33 (each $v_{1/2}$ 30 Hz)	–	−3.5 (d, br, J_{Ag-P} 244 Hz)	−3.5 (232, 271)	−2.5	–

[a] In $(CD_3)_2CO$, unless other stated.
[b] Phenyl protons of all the complexes are observed as a multiplet at δ 7.45–7.60.
[c] Two pairs of doublets arising from coupling to ^{107}Ag and ^{109}Ag.
[d] In $CDCl_3$.

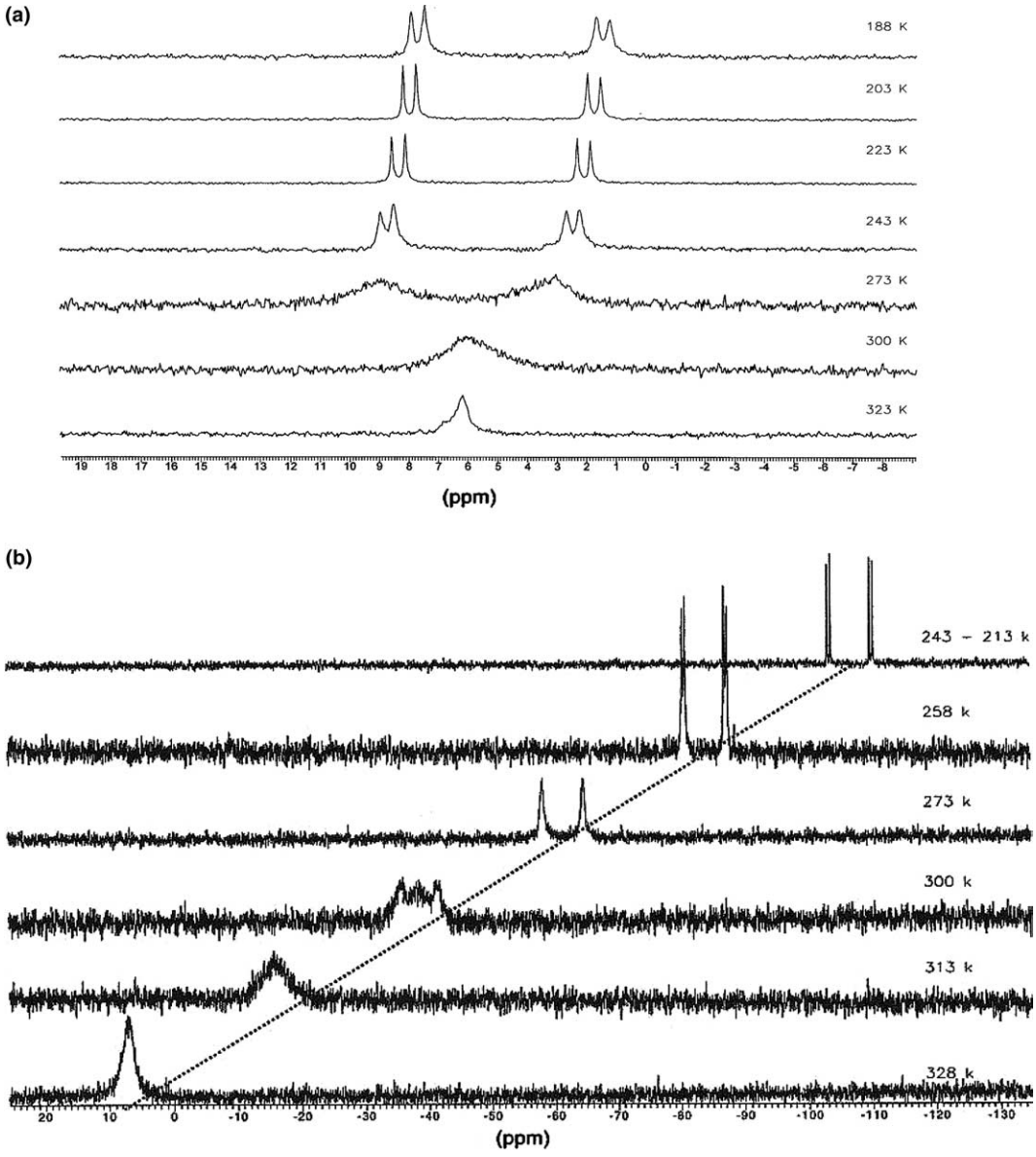

Fig. 1. VT-$^{31}P\{^1H\}$ NMR of **2** in (a) $(CD_3)_2CO$, (b) $CDCl_3$. (The scale of chemical shifts in (b) is compressed to illustrate more clearly the features of the multiplet broad peak at 300 K.)

4. Molecular structures and crystal packing

Complexes **1**–**3** with the same empirical formula, possess different structures in terms of coordination and nuclearity. X-ray diffraction analyses of the CH_2Cl_2 solvates of these complexes show that **1** and **3** are polymeric in nature. The structure of **1** comprises a two-dimensional coordination polymer, a section of which is illustrated in Fig. 2(a).

Four Ag(OTf) units are aggregated via a planar Ag_2O_2 ring ([Ag2AO22AAg2BO22B]), the centroid of which is an inversion center of symmetry. The two OTf moieties which support the Ag_2O_2 ring, each bridges (η^1-O, μ_2-O) three silver atoms, i.e. (Ag2A, Ag2B, Ag1A) and (Ag2A, Ag2B, Ag1B), respectively; whereas the other two are monodentate, each η^1-bound via O to a silver atom (Ag1A and Ag1B, respectively). These $[Ag_4(OTf)_4]$ cluster moieties are bridged by dppf ligands at all its Ag atoms, forming a two-dimensional coordination polymeric network, reinforced by C–H(Ph)···F and C–H(Cp)···O hydrogen-bonding, which also plays a role in the formation of a three-dimensional supramolecular structure (Fig. 2(b)). Bond parameters are given in Table 2. The lack of electron donors under these dppf-limiting conditions forces the Ag atoms to take up the 16-e trigonal-planar local geometry.

Complex **2** crystallizes in two different CH_2Cl_2 solvates, $\mathbf{2}\cdot CH_2Cl_2$ (**2A**) and $\mathbf{2}\cdot 0.25CH_2Cl_2$ (**2B**), which are isostructural with some variations in bond parameters, as given in Table 3. Similar to $[Ag_4(OTf)_4(PMePh_2)_4]$ [7a], **2**

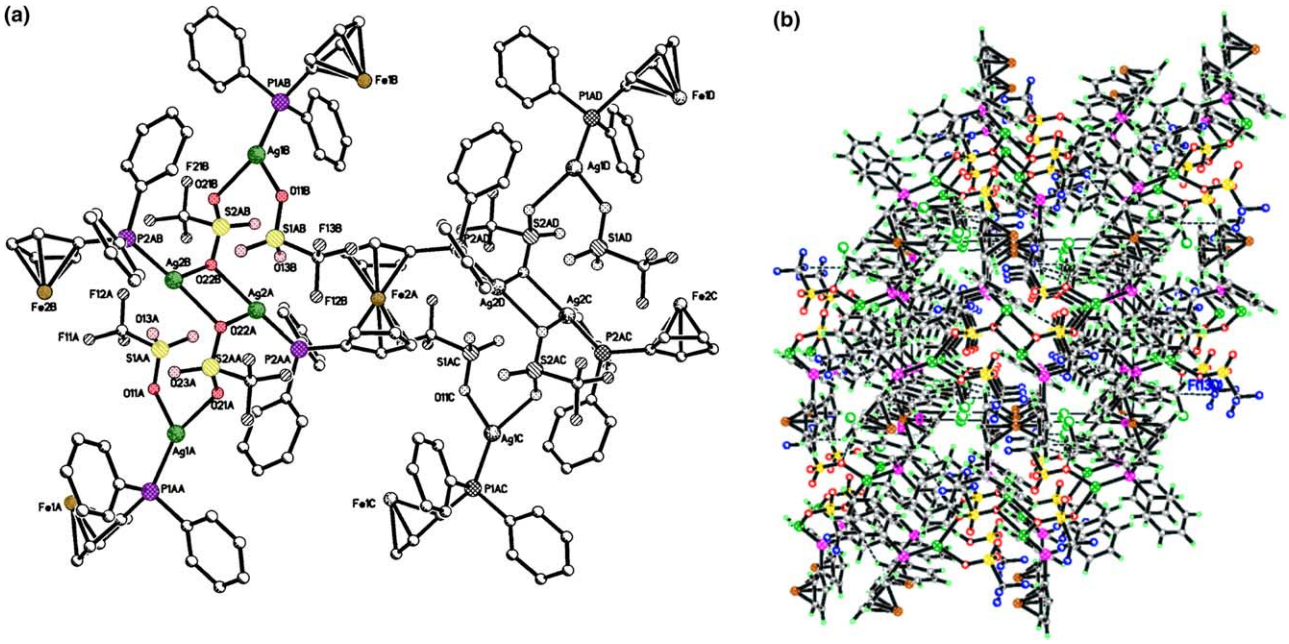

Fig. 2. (a) View of a section of the coordination polymer **1**. (b) 3-D supramolecular structure of **1**. Some H-bonding interactions are shown in dashed lines.

Table 2
Selected bond lengths (Å) and angles (°) for **1**

Bond lengths (Å)			
Ag(1)–O(1)	2.298(5)	Ag(1)–O(2)	2.333
Ag(1)–P(1)	2.3638(4)	Ag(2)–O(22)#1	2.286(4)
Ag(2)–P(2)	2.3359(15)	Ag(2)–O(22)	2.430(5)
S(1)–O(11)	1.439(6)	S(1)–O(12)	1.412(7)
S(1)–O(13)	1.440(6)	S(1)–C(1)	1.809(8)
S(2)–O(21)	1.441(5)	S(2)–O(22)	1.447(4)
S(2)–O(23)	1.420(5)	S(2)–C(2)	1.814(7)
Angles (°)			
O(11)–Ag(1)–O(12)	97.1(2)	O(11)–Ag(1)–P(1)	134.88(16)
O(21)–Ag(1)–P(1)	121.51(15)	O(22)#1–Ag(2)–P(2)	147.83(13)
O(22)#1–Ag(2)–O(22)	82.88(16)	P(2)–Ag(2)–O(22)	125.01(11)
Ag(2)#1–O(22)–Ag(2)	97.12(16)	S(1)–O(11)–Ag(1)	124.6(3)
S(2)–O(21)–Ag(1)	130.6(3)	S(2)–O(22)–Ag(2)#1	121.7(3)
C(11)#2–Fe(2)–C(11)	180.0(4)	C(15)#2–Fe(1)–C(15)	180.000(1)
C(12)#2–Fe(1)–C(12)	180.000(1)	C(13)#2–Fe(1)–C(13)	180.0(4)
C(14)#2–Fe(1)–C(14)	180.00(19)	C(21)#2–Fe(2)–C(21)	180.000(2)
C(22)#2–Fe(2)–C(22)	180.0(2)	C(25)#2–Fe(2)–C(25)	180.0(3)

Symmetry transformations used to generate equivalent atoms: #1 $-x+1, -y+1, -z+1$; #2 $-x, -y+2, -z$; #3 $-x+2, -y+1, -z+1$.

possesses a discrete tetra-silver entity, but their structures are significantly different. That of **2** contains a Ag_4 rectangular make-up, the centroid of which constitutes an inversion center (Fig. 3(a)). The four Ag atoms are symmetrically bridged by two dppf ligands and two single-anchor (O) triflates on the periphery, and cross-connected by the remaining two μ_4-triflates. This bonding mode of OTf was found in $[Ag_2(DCPA)(OTf)_2]$ (DCPA = 3,3′-dicyanodiphenylacetylene) [2j]. As seen more clearly in the line-drawing of **2** in Fig. 3(a), the asymmetric unit contains five fused metallacycles, consisting of two 'rings' of $Ag_2(dppf)O_2S$ and one each of $AgOSOAgOSO$, Ag_2O_3S and Ag_2O_2. The high level of denticity of the two μ_4-triflates results in 18-e tetrahedral Ag(I) centers. As expected, there is negligible direct Ag···Ag interactions in this tetrahedral d^{10} system. The connectivity resulting from two μ_4-triflates produces a compact structure that is markedly different from that of $[Ag_4(OTf)_4(PMePh_2)_4]$ [7a], in which pairs of Ag centers are connected by a μ-O,O′-triflate to give a 'step' configuration (Fig. 4(a)), related to the usual 'chair' geometry of many tetra-silver $Ag_4X_4L_4$ complexes (Fig. 4(b)). These differences are not related to the phosphines, as evident from similar Ag–P distances.

Table 3
Selected bond lengths (Å) and angles (°) for **2A** and **2B**

	2A	2B		2A	2B
Bond lengths (Å)					
Ag(1)–P(1)	2.3593(8)	2.3524(19)	Ag(1)–O(1)	2.454(2)	2.456(5)
Ag(2)–P(2)	2.3464(8)	2.338(2)	Ag(1)–O(3)or O(3)#1	2.583(3)	2.427(5)
Ag(2)–O(2)	2.539(2)	2.355(5)	Ag(2)–O(3) or O(3)#1	2.383(2)	2.462(6)
Ag(2)–O(4)	2.376(2)	2.416(6)	S(1)–O(1)	1.437(2)	1.437(5)
S(1)–O(2)	1.432(2)	1.435(6)	S(1)–O(3)#1 or O(3)	1.451(2)	1.448(6)
S(2)–O(4)	1.458(2)	1.456(6)	S(2)–O(5)	1.431(3)	1.403(12)
S(2)–O(6)	1.432(3)	1.399(12)	Ag(1)···Ag(2)	3.779(1)	3.846(2)
			Ag(1)···Ag(2A)	4.683(1)	4.306(2)
Angles (°)					
P(1)–Ag(1)–O(1)	135.76(6)	135.85(13)	P(1)–Ag(1)–O(4)	138.04(6)	133.43(15)
P(1)–Ag(1)–O(3) or P(1)–Ag(1)–O(3)#1	120.65(6)	126.64(14)	P(2)–Ag(2)–O(2)	119.25(6)	138.57(14)
P(2)–Ag(2)–O(4)	134.89(6)	129.13(15)	P(2)–Ag(2)–O(3) or P(2)–Ag(2)–O(3)#1	141.29(7)	123.15(13)
O(4)–Ag(1)–O(1)	77.61(8)	82.1(2)	O(4)–Ag(1)–O(3) or O(4)–Ag(1)–O(3)#1	75.38(8)	73.59(19)
O(4)–Ag(2)–O(3) or O(4)–Ag(2)–O(3)#1	78.99(8)	72.71(18)	O(4)–Ag(2)–O(2)	75.73(9)	86.0(2)
Ag(2)–O(4)–Ag(1)	105.93(9)	105.9(2)	Ag(2)–O(3)–Ag(1) or Ag(1)#1–O(3)–Ag(2)#1	99.05(8)	103.8(2)
Ag(2)–O(2)–S(1)	138.29(15)	125.7(3)	Ag(1)–O(1)–S(1)	131.19(15)	125.3(3)

O(3)#1, Ag(1)#1, Ag(2)#1 atoms are in **2B**.

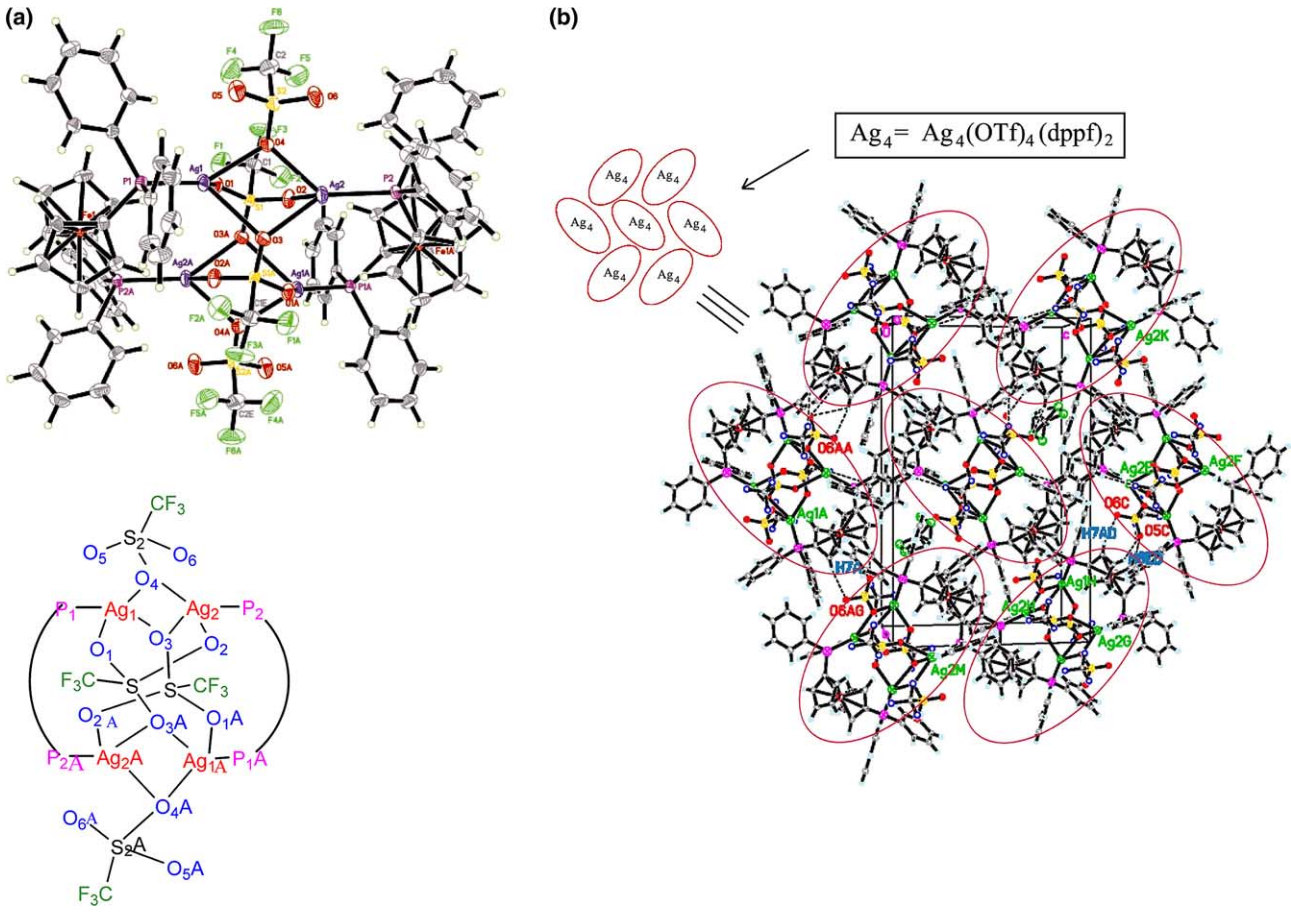

Fig. 3. (a) Molecular structure and line-drawing of **2A/2B**. Thermal ellipsoids are drawn to 50% probability level. (b) Packing diagram of **2A**, showing H-bonding (in dashed lines) between one central Ag_4 unit and six surrounding units.

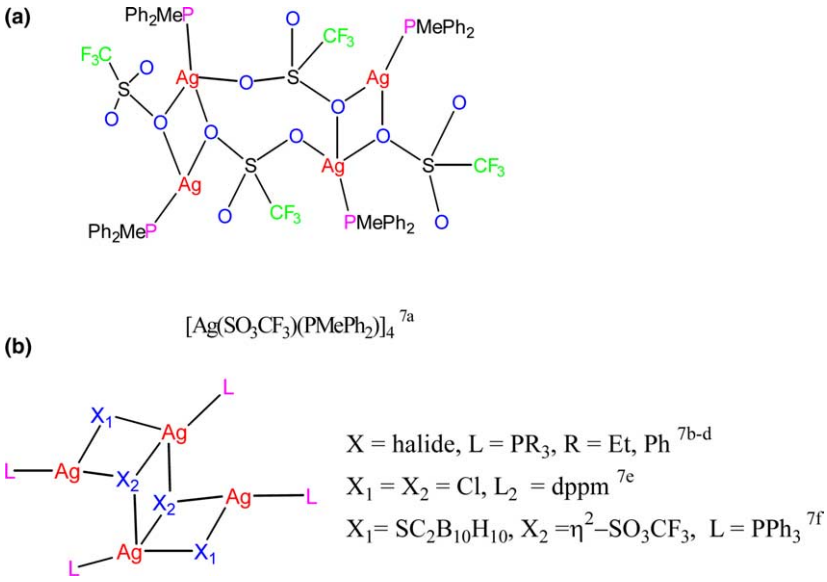

Fig. 4. (a) Line drawing of $[Ag(SO_3CF_3)(PMePh_2)]_4$. (b) Chair configuration of $Ag_4X_4L_4$ type compounds.

The geometrical flexibility of Ag(I), in an already highly complex adjustable state with mobile ligands such as triflate and dppf, makes this an ideal system for supramolecular examination. We find extensive intermolecular C–H···O and C–H···F–C hydrogen-bonding in the crystal lattices of **2A** and **2B**. The slight difference of a fractional molecule of CH_2Cl_2 in their crystal lattices is accentuated into significantly different crystal packing patterns, giving two very different supramolecular network structures. In the crystal lattice of **2A**, one central tetrameric unit is linked to six surrounding units via three types of hydrogen-bonds, involving both Cp and Ph hydrogen atoms and both ends (F and O) of a triflate, resulting in a two-dimensional network (Fig. 3(b)). The structure of **2B** consists of a 3-dimensional supramolecular network (Fig. 5(a)) formed by the linking of adjacent 'crossed' layers; the prototypes of each layer, consisting of hydrogen-bonded tetrameric units, are illustrated in Figs. S5a1 and S5a2, given in SI. Additional hydrogen-bonding interactions between two 'crossed' layers are illustrated in Fig. S5b. The contrasting features between the assemblies of **2A** and **2B** resemble those of the different network structures of $[Ag_2(DCPA)(OTf)_2]$ (DCPA = 3,3′-dicyanodiphenylacetylene) resulted from the use of different recrystallizing solvents (benzene and toluene) [2j].

Complex **3** presents a form of polymeric assembly, fundamentally different from that of **1**. Unlike **1** which has both terminal and bridging triflates, **3** has no terminal ligands. Keeping the 16-e trigonal-planar basic geometry, each Ag(I) is inter-connected by two μ_2-bridging triflates and bridging dppf. The lack of face-bridging μ_3-triflates forces the assembly to take up a more open uni-directional propagation. The basic unit of this polymeric chain is easily visualized as an eight-membered $[Ag_2S_2O_4]$ macrocyclic ring, exo-connected by bridging dppf, viz. [–(μ-dppf)Ag(μ-OTf)$_2$Ag–] (Fig. 6(a)). This coordination polymer is further strengthened by an unusually short (and presumably significant) non-bonding Ag···C interaction (Ag(1)···C(213) 2.489(6) Å) between the phenyl ring and metal. This interaction appears to give extra

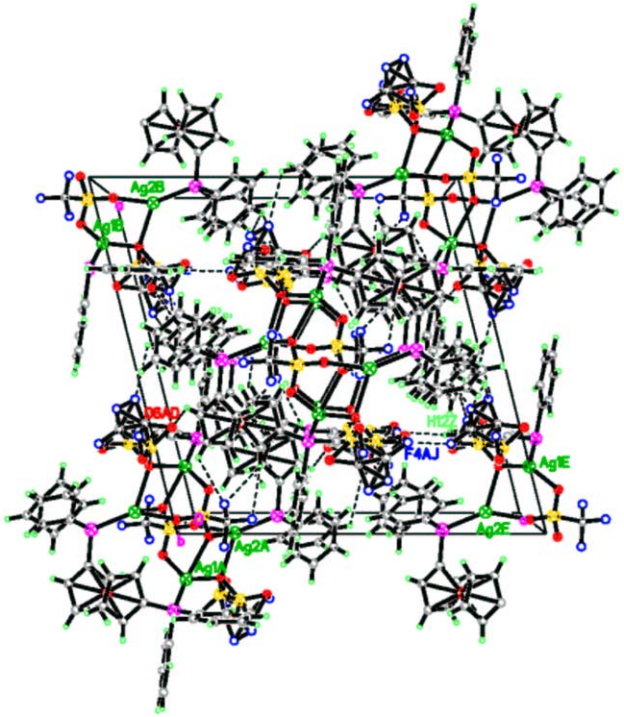

Fig. 5. (a) Packing diagram of **2B**, viewed from the *b*-axis, showing superimposition of two adjacent layers, individual illustrations of which are given in Fig.5a1 and Fig.5a2 in SI.

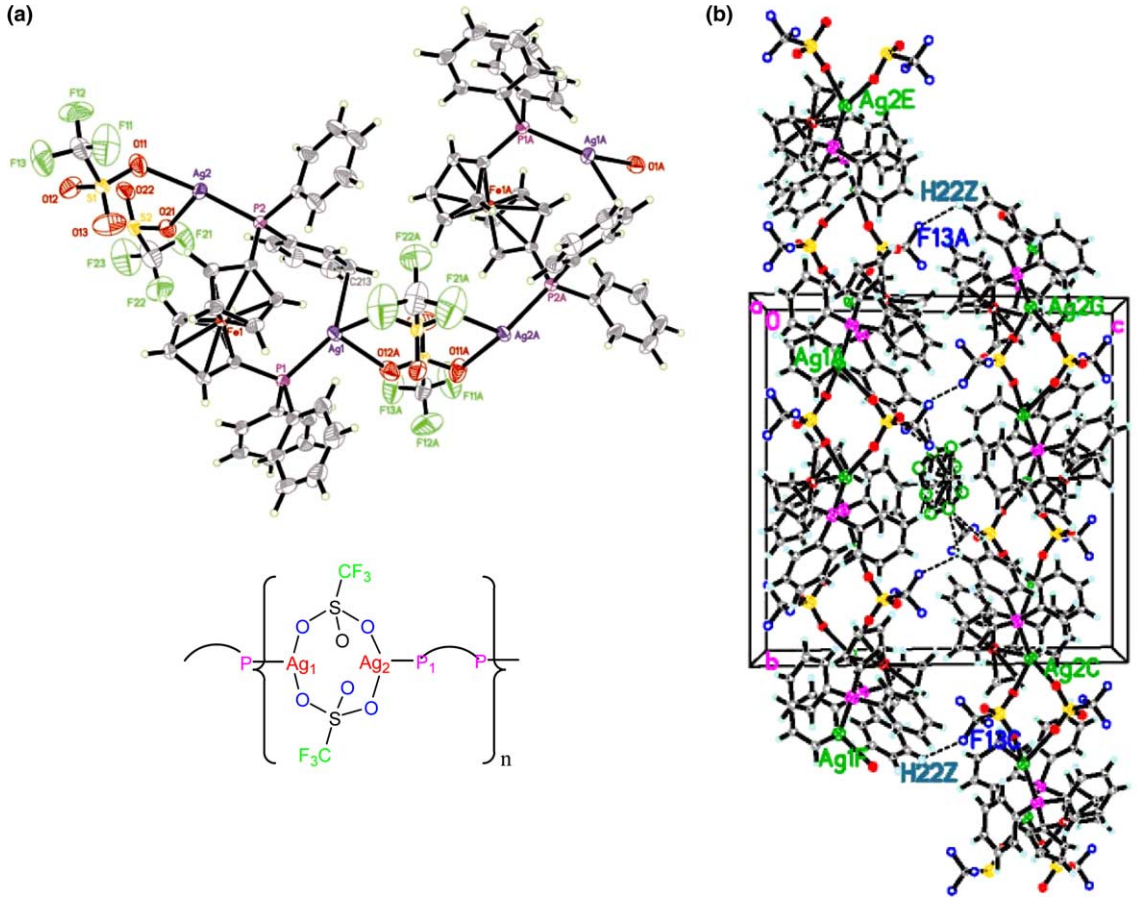

Fig. 6. (a) A view and line-drawing of the polymeric chain structure of **3**. Thermal ellipsoids are drawn to 50% probability level. (b) 3-D supramolecular structure of **3**, showing C–H(Ph)···F(OTf) H-bonds and interactions of F(OTf)with CH_2Cl_2 shown as disordered molecules in the central portion of the diagram.

support to the "unsaturated" 16-e trigonal planar Ag(I). Other selected bond parameters are given in Table 4. Unlike in **2A/2B**, the CH_2Cl_2 solvate molecule participates in weak inter-chain and inter-layer interactions with the Ph rings of dppf ligand (the weak hydrogen bonds between Cl and H(Ph) being Cl3S···H(223), 2.61 Å, 124° and Cl3S···H(224), 2.73 Å, 119° (see Table S4). A 3-D view of the polymer chain, showing H-bonding interactions is given in Fig. S6c in SI). Together with additional inter-chain H-bonding between the hydrogen atoms of Cp and Ph rings with coordinated triflate oxygen and fluorine atoms, we witness a three-dimensional supramolecular structure (Fig. 6(b)). The role of dppf in this assembly, as well as in those of **2A/2B**, seems to be critical. This is best illustrated when a bidentate dppf is replaced by two monodentate phosphines. For example, $[Ag_4(OTf)_4(PMePh_2)_4]$ [7a] adopts a completely different tetrameric, but discrete, entity in the crystalline state, as discussed above. Incidentally, the Ag···Ph interaction (Ag–C44 = 2.721(3) Å) is also apparent in this structure although it is significantly longer, and presumably weaker, than that (2.489(6) Å) in **3**.

Compound **5** is mononuclear, in which the silver atom exhibits a distorted tetrahedral coordination geometry with two chelating dppf ligands. Selected bond lengths and bond angles are given in Table 5. The structure of the molecular unit shown in Fig. 7(a), resembles that of the cation $[Ag(dppf)_2]ClO_4$, for which no secondary interactions were reported [6c]. However, in complex **5** five types of hydrogen-bonding interactions, viz. C–H(Ph)···O, C–H(CH_2Cl_2)···O, C–H(Ph)···Cl, C–H(Ph)···F and C–H(CH_2Cl_2)···F, connect CH_2Cl_2, the Ph rings of dppf and CF_3SO_3, to form a 2-D supramolecular network, shown in Fig. 7(b).

The systems discussed above demonstrate the stabilization of supramolecular assemblies via the extensive occurrence of weak secondary hydrogen-bonding interactions. Though frequently observed in organic and coordination compounds [11], these interactions in organometallic complexes have only recently been noticed [11f,12]. Here we observe bonding interactions between the C–H's of arene or Cp rings to oxygen or fluorine atoms of the CF_3SO_3 moiety. Literature examples show

Table 4
Selected bond lengths (Å) and angles (°) in **3**

Bond lengths (Å)			
Ag(1)–P(1)	2.3827(14)	Ag(2)–P(2)	2.3781(14)
Ag(1)–O(12)#1	2.414(5)	Ag(1)–O(1)	2.528(4)
Ag(2)–O(11)	2.303(5)	Ag(2)–O(21)	2.403(4)
Ag(1)–C(213)	2.489(6)	Ag(1)#2–O(12)	2.414(5)
S(1)–O(13)	1.396(6)	S(1)–O(12)	1.421(5)
S(1)–O(11)	1.436(5)	S(1)–C(1)	1.806(8)
S(2)–O(22)	1.422(5)	S(2)–O(21)	1.426(4)
S(2)–O(1)#2	1.427(4)	S(2)–C(2)	1.796(9)
C(1)–F(11)	1.292(10)	C(1)–F(12)	1.282(10)
C(1)–F(13)	1.289(9)	C(2)–F(21)	1.319(12)
C(2)–F(22)	1.301(15)	C(2)–F(23)	1.278(13)
Angles (°)			
P(1)–Ag(1)–O(12)#1	104.68(12)	P(1)–Ag(1)–C(213)	144.06(17)
O(12)#1–Ag(1)–C(213)	103.37(19)	P(1)–Ag(1)–O(1)	120.25(13)
O(12)–Ag(1)–O(1)	84.72(18)	C(213)–Ag(1)–O(1)	84.2(2)
O(11)–Ag(2)–P(2)	139.04(17)	O(11)–Ag(2)–O(21)	91.90(19)
P(2)–Ag(2)–O(21)	113.61(12)	C(221)–P(2)–Ag(2)	117.60(17)
C(211)–P(2)–Ag(2)	112.53(1)		

Symmetry transformations used to generate equivalent atoms: #1 $-x+3/2, y+1/2, -z+1/2$; #2 $-x+3/2, y-1/2, -z+1/2$.

Table 5
Selected bond lengths (Å) and bond angles (°) for **5**

Ag(1)–P(1)	2.5604(9)	Ag(1)–P(2)	2.6415(9)	Ag(1)–P(3)	2.6121(10)
Ag(1)–P(4)	2.5641(9)	P(1)–C(1)	1.806(3)	P(2)–C(6)	1.811(4)
P(3)–C(16)	1.800(3)	P(4)–C(11)	1.819(3)	P(3)–C(31)	1.821(5)
P(3)–C(32)	1.829(5)	P(1)–C(1A)	1.824(3)	P(1)–C(1B)	1.828(3)
P(2)–C(1C)	1.825(3)	P(2)–C(1D)	1.837(3)	P(3)–C(1E)	1.830(4)
P(3)–C(1F)	1.836(4)	P(4)–C(1H)	1.833(3)	P(4)–C(1G)	1.834(4)
S(1)–O(1)	1.384(4)	S(1)–O(3)	1.371(4)	S(1)–O(2)	1.404(4)
P(1)–Ag(1)–P(2)	104.91(4)	P(1)–Ag(1)–P(3)	117.99(3)		
P(1)–Ag(1)–P(4)	114.03(3)	P(4)–Ag(1)–P(3)	98.02(3)		
P(4)–Ag(1)–P(2)	106.50(3)	P(3)–Ag(1)–P(2)	115.06(3)		

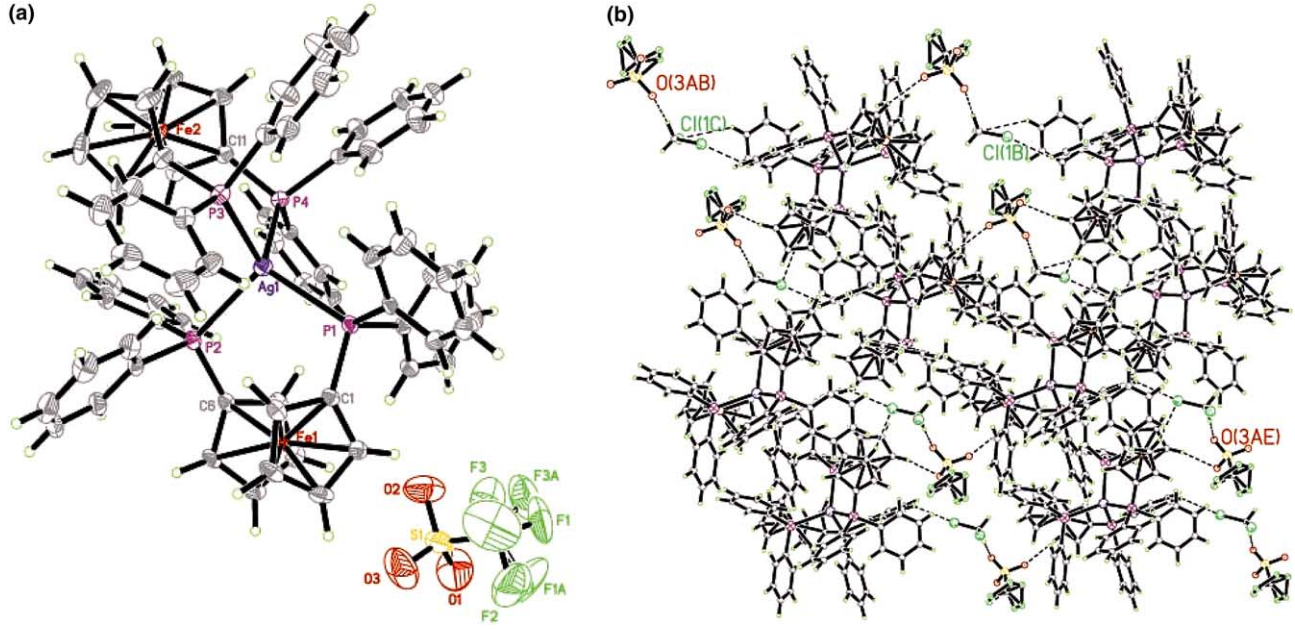

Fig. 7. (a) Molecular structure of **5**. Thermal ellipsoids are drawn to 50% probability level. (b) Packing diagram of **5**, showing C–H···O and C–H···F H-bonds (in dashed lines) between SO_3CF_3 and CH_2Cl_2 and the ring H's of Cp and Ph of dppf.

bonding of C–X(arene) to O of CO ligand for X = H [11f] or F [12c] and to F of BF_4^- [12b] or PF_6^- [12e] for X = H.

5. Conclusion

The coordination flexibility of the ligand(s) and geometric variability of the metal in a seemingly simple Ag(I)/triflate/diphosphine system has given rise to a variety of coordination and polymeric complexes. Intramolecular interactions have resulted in supramolecular assemblies which are further influenced by solvent effects.

6. Experimental

6.1. General

Ag(OTf) and dppf were used as supplied from Strem Chemicals. All reactions were performed under dry nitrogen using Schlenk techniques. Solvents were freshly distilled from standard drying agents. NMR spectra were recorded on a Bruker ACF300 FT NMR spectrometer (^{1}H at 300.13 MHz; ^{31}P{^{1}H} at 121.50 MHz and ^{19}F at 282.38 MHz), with chemical shifts referenced to residual non-deutero solvent, external H_3PO_4 and external CF_3COOH, respectively. Infrared spectra were measured in KBr pellet in the range of 400–4000 cm^{-1} on a Perkin Elmer 1600 FT-IR spectrometer. FAB mass spectra were obtained on a Finnigan MAT95XL-T spectrometers. All elemental analyses were carried out in-house.

6.2. Synthetic reactions

All NMR data are given in Table 1, whereas IR and mass spectral data are given in Table S1 in Supplementary Information.

6.2.1. (a) Using 3 Ag^+:1 dppf

(i) *1.5 h reaction.* To a suspension of Ag(OTf) (0.130 g, 0.51 mmol) in $CHCl_3$ (1 ml) was added dppf (0.097 g, 0.18 mmol) and the mixture was stirred for 1.5 h at ambient temperature. The resultant suspension was filtered to collect a yellow precipitate, which on crystallisation gave $[Ag_2(OTf)_2(dppf)]_n$ (**3**) (0.064 g, 0.060 mmol, 34% yield). Anal. Calc. for $C_{72}H_{56}F_{12}O_{12}P_4S_4Ag_4Fe_2$ (**3**)·$CHCl_3$: C, 38.8; H, 2.6; S, 5.7. Found: C, 38.8; H, 2.6; S, 5.3%. Diffraction-quality crystals of **3**·$0.5CH_2Cl_2$ were obtained from CH_2Cl_2–hexane after 1 day at ambient temperature.

Concentration of the filtrate to ca. 0.5 ml, followed by addition of hexane (1 ml) gave air-stable yellow solids of $[Ag_2(OTf)_2(dppf)]_n$ (**1**) (0.119 g, 0.11 mmol, 64% yield). Anal. Calc. for $C_{36}H_{28}F_6O_6P_2S_2Ag_2Fe$: C, 40.5; H, 2.6; S, 6.0. Found: C, 39.9; H, 2.6; S, 6.2%. Recrystallisation from CH_2Cl_2–hexane after 8 h at −15 °C yielded yellow diffraction-quality crystals of **1**·$0.5CH_2Cl_2$.

(ii) *20 h reaction*. To a suspension of Ag(OTf) (0.398 g, 1.55 mmol) in $CHCl_3$ (20 ml) was added dppf (0.289 g, 0.52 mmol) and the mixture was stirred for 20 h. The resultant suspension was filtered to collect a yellow precipitate of **3** described above (0.189 g, 0.18 mmol, 34% yield). Concentration of the filtrate to ca. 2 ml, followed by addition of hexane (3 ml) gave air-stable yellow–brown crystalline solids of $[Ag_4(OTf)_4(dppf)_2]$(**2**) (0.341 g, 0.16 mmol, 62% yield). Anal. Calc. for $C_{72}H_{56}F_{12}O_{12}P_4S_4Ag_4Fe_2$(**2**)$CHCl_3$: C, 38.8; H, 2.6; S, 5.7. Found: C, 38.6; H, 2.8; S, 5.6%. Diffraction-quality crystals of **2** were obtained as **2**·$0.25CH_2Cl_2$ (**2B**) from CH_2Cl_2–hexane after 1 day at ambient temperature.

6.2.2. (b) Using 2 Ag^+:1 dppf

To a solution of Ag(OTf) (0.103 g, 0.40 mmol) in MeOH (10 ml) was added dppf (0.111 g, 0.20 mmol) in THF (10 ml) and the mixture was stirred for 15 h at room temperature. The resultant orange suspension was filtered through Celite. Concentration of the orange–red filtrate to ca. 2 ml, followed by addition of ether (5 ml) precipitated air-stable yellow solids, which on recrystallization from CH_2Cl_2–hexane gave $[Ag_4(SO_3CF_3)_4(dppf)_2]$ (**2**) (0.073g, 72% yield). Anal. Calc. for $C_{72}H_{56}F_{12}O_{12}P_4S_4Ag_4Fe_2$: C, 40.5; H, 2.6; P, 5.8; F, 10.7. Found: C, 40.7; H, 2.6; P, 6.2; F, 9.5%. Diffraction-quality crystals of **2**·CH_2Cl_2 (**2A**) were obtained from this sample after 3 days by slow evaporation of a solution in CH_2Cl_2 at room temperature.

6.2.3. (c) Using 1 Ag^+:1 dppf in CH_2Cl_2

To a suspension of Ag(OTf) (0.055 g, 0.21 mmol) in CH_2Cl_2 (10 ml) was added dppf (0.119 g, 0.21 mmol) in toluene (10 ml) and the mixture stirred for 8 h. This was filtered to give a yellow solution, which on concentration to 1 ml followed by addition of hexane (2 ml), gave yellow solids of [Ag(dppf)(OTf)] (**4**) (0.153 g, 0.19 mmol, 90%). Anal. Calc. for $C_{35}H_{28}F_3O_3P_2SAgFe$: C, 51.8; H, 3.5; S, 3.9. Found: C, 51.8; H, 3.5; S, 3.8%. The structure has not been solved because of disorder.

6.2.4. (d) Using 1 Ag^+:2 dppf

To a solution of Ag(OTf) (0.055 g, 0.22 mmol) in MeOH (10 ml) was added a THF solution (10 ml) of dppf (0.222 g, 0.40 mmol) and the mixture stirred for 8 h. This was filtered through celite to obtain an orange filtrate, which was concentrated to ca. 2 ml; addition of ether (5 ml), gave yellow solids of $[Ag(dppf)_2](OTf)$ (**5**) (0.264 g, 90%). Anal. Calc. for $C_{69}H_{56}F_3O_3P_4SAgFe_2$: C, 60.7; H, 4.1; S, 2.4; P, 9.1; F, 4.2. Found: C, 60.6; H, 4.2; S, 2.5; P, 8.3; F, 4.2%.

7. X-ray diffraction analyses

Crystals were obtained as described above and mounted on a quartz fibre. X-ray data were collected on a Bruker SMART APEX diffractometer, equipped with a CCD detector, using Mo K_α radiation at ambient 223 K. Data were corrected for Lorentz and polarisation effects with the SMART suite of programs [13], and for absorption effects with SADABS [14]. Structural solution and refinement were carried out with the SHELXTL suite of programs [15].

The structures were solved by direct methods to locate the heavy atoms, followed by difference maps for the light, non-hydrogen atoms. The aromatic hydrogens were placed in calculated positions. All non-hydrogen atoms were generally given anisotropic displacement parameters in the final model (but see below). For **1**, the CH_2Cl_2 solvent molecule was modeled as disordered over three sites, all atoms isotropic, with occupancies of 0.2, 0.2 and 0.1. For **2A**, the CH_2Cl_2 solvent molecule was modeled as disordered over two sites with occupancies of 0.65 and 0.35. For **2B**, there was disorder of one of the triflate groups. This was modeled as disordered over two sites, with occupancies summing to unity. The S atoms were allowed to refine anisotropically; the lighter atoms were given common isotropic thermal parameters. Appropriate restraints were placed on bond parameters. There was also a half-molecule of CH_2Cl_2 solvent which was disordered about a centre of symmetry. This was also modeled with an isotropic model, with restraints on bond parameters. For **3**, the half molecule of CH_2Cl_2 solvent was modeled as disordered over two sites, with occupancies of 0.4 and 0.1. For **5**, a CH_2Cl_2 solvent molecule was found; the C–Cl bond lengths were restrained to be the same. Details of crystal parameters, data collection and structure refinement are summarized in Table S6 in SI. Bond parameters of complexes **1**, **2A**, **2B**, **3** and **5**, are given in Tables 2–5 and their respective H-bonding parameters in Tables S2–S5 in SI.

8. Supplementary information available

Figs. S5a1 and S5a2 showing the 'cross' layers in the supramolecular structure of **2B**. Fig. S5b showing two adjacent superimposed layers in the supramolecular structure of **2B**. Fig. S6c giving a 3-D view of the linear polymeric chain structure of **3**. Table S1 giving IR and mass spectral data. Tables S2–S5 giving H-bond parameters of the complexes. Table S6 giving details of crystal parameters, data collection and structure refinement. Crystallographic data for **1**, **2A**, **2B**, **3** and **5** have been deposited at the Cambridge Crystallographic Data Centre with deposition numbers 197937, 197934, 197936, 197935 and 214937, respectively. Copies of the information may be obtained free of charge from The Director, CCDC, 12 Union Road, Cambridge CB2 1EZ, UK (Fax: +44-1223-336033; e-mail: deposit@ccdc.cam.ac.uk or http://www.ccdc.cam.ac.uk).

Acknowledgements

Support from the National University of Singapore as Academic Research Fund Grant Nos. R14300077112 and R14300135112 to L.Y.G and a research scholarship to X.L.L is gratefully. We also thank Prof. Philip A.W. Dean (University of Western Ontario, Canada) for helpful discussions, Ms. G.K. Tan, Dr. Koh and Dr. B.W. Sun for technical assistance.

References

[1] (a) J.C. Noveron, M.S. Lah, R.E. Del Sesto, A.M. Arif, J.S. Miller, P.J. Stang, J. Am. Chem. Soc. 124 (2002) 6613;
(b) M. Eddaoudi, D.B. Moler, H. Li, B. Chen, T.M. Reineke, M. O'Keeffe, O.M. Yaghi, Acc. Chem. Res. 34 (2001) 319;
(c) S. Leininger, B. Olenyuk, P.J. Stang, Chem. Rev. 100 (2000) 853;
(d) P.J. Hagrman, D. Hagrman, J. Zubieta, Angew. Chem. Int. Ed. 38 (1999) 2638;
(e) A.J. Blake, N.R. Champness, P. Hubberstey, W.-S. Li, M.A. Withersby, M. Schröder, Coord. Chem. Rev. 183 (1999) 117;
(f) S.R. Batten, R. Robson, Angew Chem. Int. Ed. 37 (1998) 1460;
(g) D.L. Caulder, K.N. Raymond, Acc. Chem. Res. 32 (1999) 975;
(h) C.B. Aakeröy, A.M. Beatty, Chem. Commun. (1998) 1067;
(i) D. Braga, F. Grepioni, G.R. Desiraju, Chem. Rev. 98 (1998) 1375;
(j) P.J. Stang, Chem. Eur. J. 4 (1998) 19;
(k) P.J. Stang, B. Olenyuk, Acc. Chem. Res. 30 (1997) 502;
(l) G.M. Whitesides, J.P. Mathias, C.T. Seto, Science 254 (1991) 1312.

[2] (a) B.H. Hamilton, C.J. Xiegler, Chem. Commun. (2002) 842, G.K. Patra, I. Goldberg, J. Chem. Soc., Dalton Trans. (2002) 1051;
(b) D.M.L. Goodgame, D.A. Grachvogel, D.J. Williams, J. Chem. Soc., Dalton Trans. (2002) 2259;
(c) B. Schmaltz, A. Jouaiti, M.W. Hosseini, A.D. Cian, Chem. Commun. (2001) 1242;
(d) Y. Kang, Y.S.S. Lee, K.-M. Park, S.H. Lee, S.O. Kang, J. Ko, Inorg. Chem. 40 (2001) 7027;
(e) S.-L. Zheng, M.-L. Tong, X.-L. Yu, X.-M. Chen, J. Chem. Soc., Dalton Trans. (2001) 586;
(f) Y. Suenaga, T. Kuroda-Sowa, M. Maekawa, M. Munakata, J. Chem. Soc., Dalton Trans. (2000) 3620;
(g) W. Su, M. Hong, J. Weng, R. Cao, S. Lu, Angew. Chem. Int. Ed. 39 (2000) 2911;
(h) L. Carlucci, G. Ciani, P. Macchi, D.M. Proserpio, S. Rizzato, Chem. Eur. J. 5 (1999) 237;
(i) K.A. Hirsch, S.R. Wilson, J.S. Moore, J. Am. Chem. Soc. 119 (1997) 10401;
(j) K.A. Hirsch, S.R. Wilson, J.S. Moore, Inorg. Chem. 36 (1997) 2960;
(k) D. Venkataraman, S. Lee, J.S. Moore, P. Zhang, K.A. Hirsch, G.B. Gardner, A.C. Covey, C.L. Prentice, Chem. Mater. 8 (1996) 2030;
(l) L. Carlucci, G. Ciani, D.M. Proserpio, A. Sironi, J. Am. Chem. Soc. 117 (1995) 4562.

[3] S.J. Berners-Price, R.J. Bowen, P. Galettis, P.C. Healy, M.J. McKeage, Coord. Chem. Rev. 823 (1999) 185–186.
[4] M. Ohkouchi, D. Masui, M. Yamaguchi, T. Yamagishi, J. Mol. Catal. A: Chem. 170 (2001) 1.
[5] (a) D. Sun, R. Cao, J. Weng, M. Hong, Y. Liang, J. Chem. Soc., Dalton Trans. (2002) 291;
(b) C.-M. Che, M.-C. Tse, M.C.W. Chan, K.-K. Cheung, D.L. Philips, K.-K. Leung, J. Am. Chem. Soc. 122 (2000) 2464;
(c) M.-C. Brandys, M.C. Jennings, R.J. Puddephatt, J. Chem. Soc., Dalton Trans. (2000) 4601;
(d) M.J. Irwin, J.J. Vittal, R.J. Puddephatt, Organometallics 16 (1997) 3541.
[6] (a) T.S.A. Hor, K.S. Gan, in: A. Togni, T. Hayashi (Eds.), Ferrocene – Homogeneous Catalysis, Organic Synthesis, Material Science, VCH, Weiheim, 1995 (Chapters 1 and 3);
(b) G. Bandoli, A. Dolmella, Coord. Chem. Rev. 209 (2000) 161;
(c) M.C. Gimeno, P.G. Jones, A. Laguna, C. Sarroca, J. Chem. Soc., Dalton Trans. (1995) 1473;
(d) S.-P. Neo, T.S.A. Hor, Z.-Y. Zhou, T.C.W. Mak, J. Organomet. Chem. 464 (1994) 113;
(e) T.S.A. Hor, S.-P. Neo, C.S. Tan, T.C.W. Mak, K.V.P. Leung, R.-J. Wang, Inorg. Chem. 31 (1992) 4510.
[7] (a) N. Bardají, O. Crespo, A. Laguna, A.K. Fischer, Inorg. Chim. Acta 304 (2000) 7;
(b) G. Wilkinson, R.D. Gillard, J.A. McCleverty, in: Comprehensive Coordination Chemistry, vol. 5, Pergamon, Oxford, 1987, p. 798;
(c) M.D. Churchil, J. Donahue, F.J. Rotella, Inorg. Chem. 15 (1976) 2752;
(d) B.-K. Teo, J.C. Calabrese, Inorg. Chem. 15 (1976) 2467, J. Chem. Soc., Chem. Commun. (1976) 185;
(e) P.A. Pérez-Lourido, J.A. Cracía-Vazquez, J. Romero, M.S. Louro, A. Sousa, A.Q. Chen, Y. Chang, J. Zubieta, J. Chem. Soc., Dalton Trans. (1996) 2047;
(f) M.M. Artigas, O. Crespo, M.C. Gimeno, P.G. Jones, A. Laguna, M.D. Villacampa, Inorg. Chem. 36 (1997) 6454.
[8] (a) E. Lozano, M. Nieuwenhuyzen, S.L. James, Chem. Eur. J. 7 (2001) 2644;
(b) M.-C. Brandys, R.J. Puddephatt, Chem. Commun. (2001) 1508;
(c) M.-C. Brandys, R.J. Puddephatt, J. Am. Chem. Soc. 124 (2002) 3946;
(d) F. Bachechi, A. Burini, R. Galassi, B.R. Pietroni, D. Tesei, Eur. J. Inorg. Chem. (2002) 2086.
[9] (a) E.L. Muetterties, C.W. Alegranti, J. Am. Chem. Soc. 84 (1972) 6386;
(b) R.G. Goel, P. Pilon, Inorg. Chem. 17 (1978) 2876.
[10] P.A.W. Dean, J.J. Vittal, R.S. Srivastava, Can. J. Chem. 65 (1987) 2638.
[11] (a) D. Braga, F. Grepioni, G.R. Desiraju, Chem. Rev. (1998) 1375;
(b) V.R. Thalladi, H.-C. Weiss, D. Bläser, R. Boese, A. Nangia, G.R. Desiraju, J. Am. Chem. Soc. 120 (1998) 8702;
(c) D. Braga, F. Grepioni, K. Biradha, V.R. Pedireddi, G.R. Desiraju, J. Am. Chem. Soc. 117 (1995) 3156;
(d) T. Spaniel, H. Gorls, J. Scholz, Angew. Chem. Int. Ed. 37 (1998) 1862;
(e) W. Huang, S. Gou, D. Hu, S. Chantrapromma, H.-K. Fun, Q. Meng, Inorg. Chem. 41 (2002) 864;
(f) L. Brammer, J.C.M. Rivas, R. Atencio, S. Fang, F.C. Pigge, J. Chem. Soc., Dalton Trans. (2000) 3855.
[12] (a) G.R. Desiraju, Acc. Chem. Res. 29 (1996) 441;
(b) D.L. Reger, R.F. Semeniuc, M.D. Smith, J. Chem. Soc., Dalton Trans. (2002) 476;
(c) M.P. Thornberry, C. Slebodnick, P.A. Deck, F.R. Fronczek, Organometallics 19 (2000) 5352;
(d) D. Braga, L. Maini, F. Grepioni, Angew. Chem. Int. Ed. 37 (1998) 2240;
(e) F. Grepioni, G. Cojazzi, S.M. Draper, N. Scully, D. Braga, Organometallics 17 (1998) 296.
[13] SMART & SAINT Software Reference manuals, version 5.0, Bruker AXS Inc., Madison, WI, 1998.
[14] G.M. Sheldrick, SADABS software for empirical absorption correction, University of Göttingen, Germany, 2000.
[15] SHELXTL Reference Manual, version 5.1, Bruker AXS Inc., Madison, WI, 1998.